

High-Accuracy Emissivity Data on the Coatings Nextel 811-21, Herberts 1534, Aeroglaze Z306 and Acktar Fractal Black

A. Adibekyan¹ · E. Kononogova¹ · C. Monte¹ · J. Hollandt¹

Received: 2 September 2016 / Accepted: 6 March 2017 / Published online: 8 April 2017
© The Author(s) 2017. This article is an open access publication

Abstract The Physikalisch-Technische Bundesanstalt determined the directional spectral emissivities of several widely used black coatings: Nextel 811-21, Herberts 1534, Aeroglaze Z306 and Acktar Fractal Black. These are and were often applied in different industrial and scientific applications. The measurements are taken angularly resolved over a range from 10° to 70°. They cover the temperature range typical for the application of the respective coating and a wide wavelength range from 4 μm to 100 μm. The respective directional total emissivities and hemispherical total emissivities are given as well. The measurements were taken under vacuum at the reduced background calibration facility to achieve low uncertainties and avoid atmospheric interferences. Additionally, some measurements were taken with the emissivity measurement setup in air.

Keywords Acktar Fractal Black · Aeroglaze Z306 · Black coating · Emissivity · Herberts 1534 · Nextel 811-21 · Uncertainty

Selected Papers of the 13th International Symposium on Temperature, Humidity, Moisture and Thermal Measurements in Industry and Science.

Electronic supplementary material The online version of this article (doi:[10.1007/s10765-017-2212-z](https://doi.org/10.1007/s10765-017-2212-z)) contains supplementary material, which is available to authorized users.

✉ A. Adibekyan
albert.adibekyan@ptb.de

¹ Physikalisch-Technische Bundesanstalt (PTB), Berlin, Germany

Abbreviations

CCT	Consultative committee for thermometry
DLaTGS	Deuterated L-alanine-doped triglycine sulfate
EMAF	Emissivity measurement in air facility
FDTGS	FIR deuterated triglycine sulfate
FIR	Far-infrared wavelength range
IR-FTS	Infrared Fourier transform spectrometer
ITS-90	International Temperature Scale of 1990
KBr	Potassium bromide
LN ₂	Liquid nitrogen
MCT	Liquid nitrogen-cooled mercury cadmium telluride
MIR	Mid-infrared wavelength range
PRT	Platinum resistance thermometer
PTB	Physikalisch-Technische Bundesanstalt
RBCF	Reduced background calibration facility

1 Introduction

Black coatings featuring a high emissivity corresponding to a low reflectivity from the visible to the far-infrared spectral range are widely used in optical instruments to reduce stray light, in control panels or automotive instrumentation to enhance contrast and readability, in thermal applications to control and maximize radiative cooling or heating, in spectroscopy as reference surfaces and radiance standards. For these applications, reliable data of their optical properties are mandatory. However, emissivity data of black coatings published in the literature or in standardization documents often do not provide angularly and/or spectrally resolved information and/or lack uncertainties. The Physikalisch-Technische Bundesanstalt (PTB) determined the directional spectral and directional total emissivities under several angles of observation and also the hemispherical total emissivities of several widely used diffuse black coatings: Nextel 811-21, Herberts 1534, Aeroglaze Z306 and Aektar Fractal Black.

2 Measurements Scheme

The measurements were taken under vacuum (at a pressure of 10^{-6} hPa) at the reduced background calibration facility (RBCF) [1,2] of PTB to achieve low uncertainties and avoid atmospheric interferences. Furthermore, some of the measurements are compared with measurements obtained with the emissivity measurement in air facility (EMAF) [3], which is routinely operated at PTB for several years. The EMAF successfully took part in an international emissivity comparison organized by the consultative committee for thermometry (CCT) [4].

The measurement scheme for the determination of the emissivity is a comparison of the spectral radiance of the sample which is mounted on a heater and placed inside a temperature-stabilized spherical enclosure against the spectral radiances of two reference blackbodies at different temperatures [1–3]. The comparison is performed with an

infrared Fourier transform spectrometer (IR-FTS). By using two reference blackbodies at different temperatures, the residual background radiation of the instrumentation can be corrected. The “main” reference blackbody is usually operated at a temperature close to the radiance temperature of the sample to achieve a similar signal level. The second reference blackbody is operated at a temperature significantly lower than the temperature of the main blackbody. At the RBCF, this is an liquid nitrogen-cooled (LN_2) blackbody, which is operated at the temperature of boiling nitrogen. At the EMAF, the second reference blackbody is a liquid-cooled blackbody operated at 18 °C.

3 Measurement Uncertainty

The calculation of the emissivity from the measured detector signals is based on the complete radiation budget, considering every radiation contribution in the optical path. The uncertainty of the directional spectral emissivity is calculated via a Monte–Carlo method [5, 6] based on the final determination equation of the directional spectral emissivity and is spectrally dependent. Furthermore, the uncertainty budget is calculated for each individual measurement, since the relevance of the individual uncertainty contributions depends significantly on the conditions of the measurement and the sample investigated. A detailed description of the data evaluation procedure and the uncertainty calculation is given in [6, 7].

4 Experimental Results on Different Black Coatings

The emissivity measurements of the black coatings were taken at two setups at PTB—under vacuum at the RBCF and in air at the EMAF—by applying the measurement schemes and data, and uncertainty evaluation described shortly above and described in detail in [1–3, 6, 7]. Two sets of detectors and beamsplitters were used with the IR-FTS according to the wavelength and temperature range of the measurements. In the range from 4 μm to 20 μm , a deuterated L-alanine-doped triglycine sulfate (DLaTGS) or liquid nitrogen-cooled mercury cadmium telluride (MCT) detector in combination with a potassium bromide (KBr) beamsplitter were used. Due to its higher responsivity, the MCT was used for the measurements at lower sample temperatures. In the range from 14 μm to 100 μm , the emissivity was determined by using a far-infrared deuterated triglycine sulfate (FDTGS) detector in combination with a 6 μm Multilayer Mylar beamsplitter.

Each of the investigated black coatings—Nextel 811-21, Herberts 1534, Aeroglaze Z306 and Acktar Fractal Black—was applied to copper substrates. The disk-shaped substrates have a diameter of 90 mm and a thickness of 5 mm and feature a hole of 2 mm diameter and 50 mm depth from the circumference to accommodate a platinum resistance thermometer (PRT) temperature sensor for monitoring the substrate temperature. The surface of the copper substrates was plane and untreated.

In the following, the individual emissivity results for the four different coatings are presented.

4.1 Nextel 811-21

Nextel 811-21 was in the past provided by 3M and is now available from “Mankiewicz Gebr. & Co” [8] where we obtained it. The substrates were coated according to the manufactures instructions, i.e., spray coating of the primer and spray coating of the Nextel 811-21 coating and subsequent heating at 120 °C. Some of the emittance properties of Nextel 811-21 are already provided in the literature [9,10]. Here, the spectral emissivity of the sample Nextel 811-21 was determined under vacuum in the wavelength range from 5 μm to 20 μm at a temperature of 120 °C under different angles of observation. The resulting spectral curves are plotted in Fig. 1. Some of the measured angles are omitted here for clarity of the figure. The spectrally integrated directional total emissivities are shown in the inset of Fig. 1 with their corresponding standard uncertainties. A theoretical model based on Fresnel equations is fitted to these values and plotted as a solid line. Its integration over the angular range from 0° to 90° yields the hemispherical total emissivity. A decrease in the directional spectral emissivities and accordingly of the directional total emissivities toward larger angles is clearly visible, which is typical for high-emitting samples. The numerical values of the directional total and hemispherical total emissivities of Nextel 811-21 in the wavelength range from 5 μm to 20 μm at temperature of 25 °C and from 4 μm to 20 μm at temperature of 120 °C are provided in Table 1. Within the uncertainty of the measurements, no significant spectral change in emissivity can be observed between 25 °C and 120 °C.

The directional spectral emissivity of Nextel 811-21 from 20 μm to 100 μm at a temperature of 120 °C observed under an angle of 10° is plotted in Fig. 2. The shaded area around the curve is the range of the standard uncertainty of the measurement. The

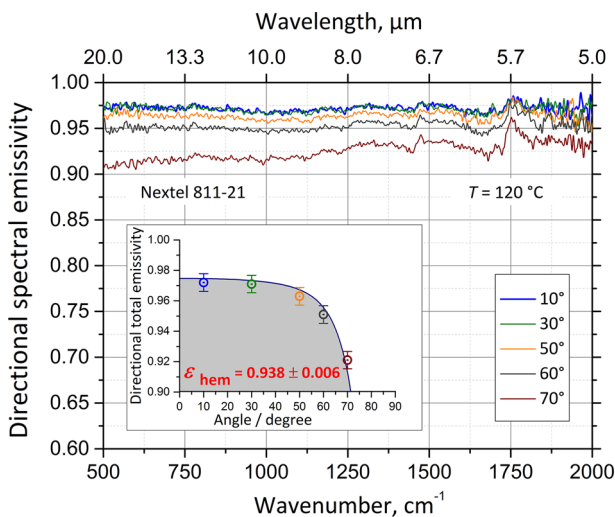


Fig. 1 Directional spectral emissivity of Nextel 811-21 measured at a temperature of 120 °C for different angles of observation. The spectrally integrated values of the directional total emissivity with their standard uncertainties as well as the hemispherical total emissivity are shown in the inset

Table 1 Directional total and hemispherical total emissivities of Nextel 811-21 in the wavelength range from 5 μm to 20 μm at 25 °C and from 4 μm to 20 μm at 120 °C with their corresponding standard uncertainties

Angle	Nextel 811-21 ϵ (25 °C)	$u(\epsilon)$ ($k=1$)	Nextel 811-21 ϵ (120 °C)	$u(\epsilon)$ ($k=1$)
10°	0.971	0.012	0.9717	0.0058
20°	0.971	0.013	0.9719	0.0057
30°	0.971	0.013	0.9685	0.0057
40°	0.966	0.012	0.9684	0.0057
50°	0.966	0.012	0.9609	0.0058
60°	0.949	0.012	0.9518	0.0058
70°	0.912	0.013	0.9168	0.0057
ϵ_{hem}	0.941	0.012	0.9381	0.0056

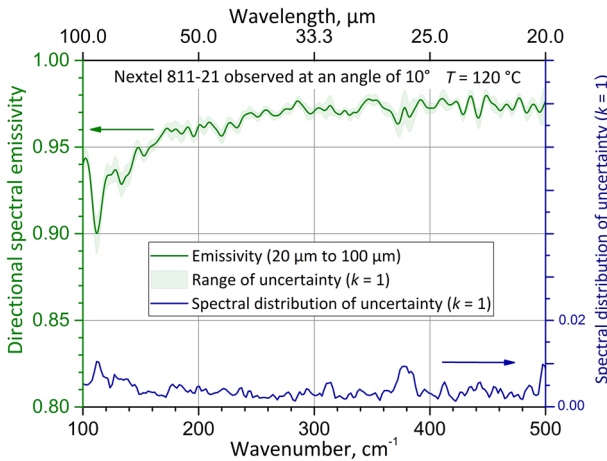


Fig. 2 Directional spectral emissivity of Nextel 811-21 up to a wavelength of 100 μm measured at a temperature of 120 °C and under an angle of observation of 10° with respect to the surface normal. The spectral distribution of the standard uncertainty is shown in the lower part of the plot with the respective scale on the right-hand ordinate axis

Table 2 Directional total and hemispherical total emissivities of Nextel 811-21 in the wavelength range from 20 μm to 100 μm with their corresponding standard uncertainties

Angle	Nextel 811-21 ϵ (120 °C)	$u(\epsilon)$ ($k=1$)
10°	0.9712	0.0038
30°	0.9689	0.0036
50°	0.9579	0.0038
70°	0.8947	0.0048
ϵ_{hem}	0.9378	0.0039

blue curve in the lower part of the graph and the corresponding right-hand ordinate axis show the spectral distribution of the uncertainty. The numerical values of the directional total and hemispherical total emissivities of Nextel 811-21 in the wavelength range from 20 μm to 100 μm are provided in Table 2.

4.2 Herberts 1534

Herberts 1534 is no longer in production but was used in the past for the far-infrared wavelength range (FIR) and space applications. There are still a number of instrumentations and blackbodies in use which are coated with this paint. Here, the spectral emissivity of the sample Herberts 1534 was measured under vacuum at a temperature of 25 °C and in air at a temperature of 120 °C and is plotted in Fig. 3. The brown curve, with its range of standard uncertainty given as a shaded area, shows the directional spectral emissivity under vacuum. Additionally, the uncertainty is also shown separately with the blue curve in the lower part of Fig. 3 and the corresponding right-hand ordinate axis. The green curve in Fig. 3 shows the directional spectral emissivity measured in air at a temperature of 120 °C. The directional spectral emissivity of Herberts 1534 measured in the wavelength range from 14.5 μm to 100 μm and, for comparison, the results obtained in the mid-infrared wavelength (MIR) range are given in Fig. 4. The results of both measurements in the overlapping spectral range from 14.5 μm to 18 μm are consistent within the range of their standard uncertainties. The numerical values of the directional total and hemispherical total emissivities are presented in Tables 3 and 4.

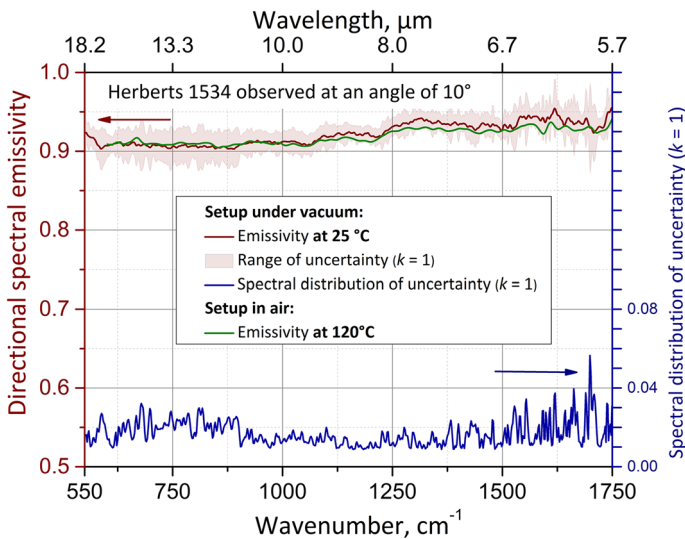


Fig. 3 Directional spectral emissivity of Herberts 1534 in the wavelength range from 5.7 μm to 18.2 μm measured at a temperature of 120 °C in air and at a temperature of 25 °C under vacuum. Both measurements were taken under an angle of observation of 10° with respect to the surface normal. The spectral distribution of the standard uncertainty of measurement at 25 °C under vacuum is shown in the lower half of the plot with the respective scale on the right-hand ordinate axis

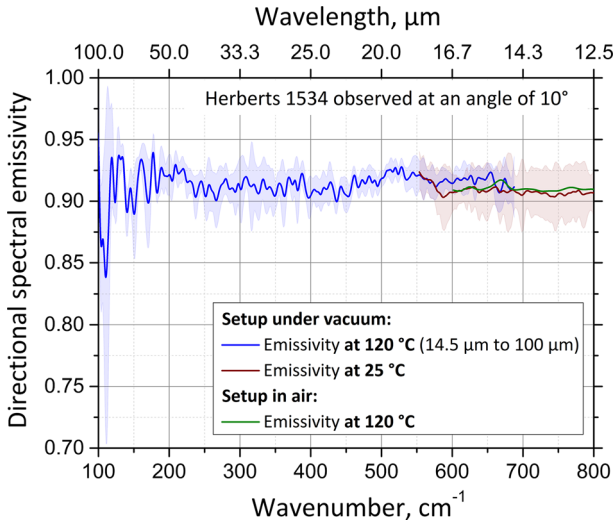


Fig. 4 Directional spectral emissivity of Herberts 1534 measured under vacuum up to a wavelength of 100 μm and compared in the overlapping wavelength range with measurements obtained under vacuum and in air in the MIR range

Table 3 Directional total and hemispherical total emissivities of Herberts 1534 in the wavelength range from 5 μm to 18.2 μm at 25 $^\circ\text{C}$ and from 4 μm to 20 μm at 120 $^\circ\text{C}$ with their corresponding standard uncertainties

Angle	Herberts 1534 ϵ (25 $^\circ\text{C}$)	$u(\epsilon)$ ($k=1$)	Herberts 1534 ϵ (120 $^\circ\text{C}$)	$u(\epsilon)$ ($k=1$)
10 $^\circ$	0.917	0.022	0.918	0.024
20 $^\circ$	0.915	0.021	0.916	0.027
30 $^\circ$	0.918	0.021	0.918	0.025
40 $^\circ$	0.916	0.021	0.917	0.024
50 $^\circ$	0.887	0.021	0.906	0.024
60 $^\circ$	0.883	0.021	0.891	0.024
70 $^\circ$	0.843	0.021	0.859	0.025
ϵ_{hem}	0.880	0.021	0.900	0.024

Table 4 Directional total and hemispherical total emissivities of Herberts 1534 in the wavelength range from 14.1 μm to 100 μm with their corresponding standard uncertainties

Angle	Herberts 1534 ϵ (120 $^\circ\text{C}$)	$u(\epsilon)$ ($k=1$)
10 $^\circ$	0.915	0.013
30 $^\circ$	0.928	0.012
50 $^\circ$	0.906	0.013
70 $^\circ$	0.842	0.014
ϵ_{hem}	0.888	0.013

4.3 Aeroglaze Z306

The Aeroglaze Z306 is an absorptive polyurethane coating which is often used in aerospace applications and which is well suited for vacuum conditions. Some of its emittance properties can be found in [11, 12]. In preparation of the measurements of Aeroglaze Z306, three copper substrates were spray coated with Aeroglaze according to the instructions given in the European Cooperation for Space Standardization

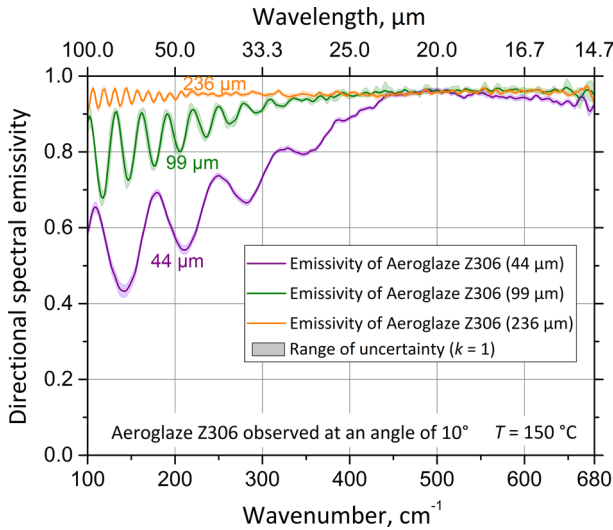


Fig. 5 Directional spectral emissivities of three Aeroglaze Z306 samples with thicknesses of 44 μm , 99 μm and 236 μm on polished copper substrates under an angle of observation of 10°

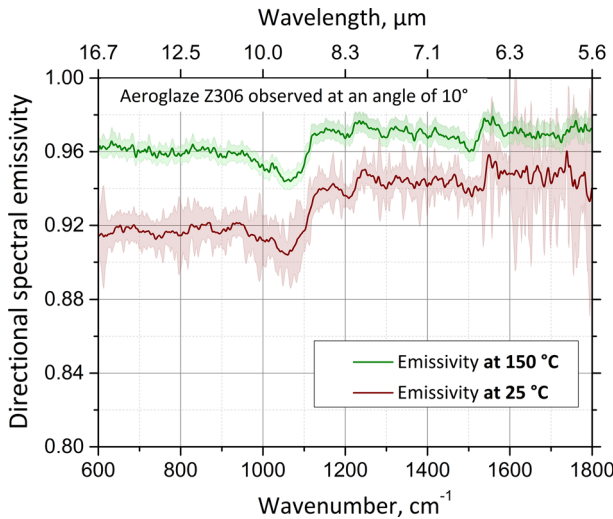


Fig. 6 Directional spectral emissivities of Aeroglaze Z306 sample with thickness of 99 μm under an angle of observation of 10° at temperatures of 25°C and 150°C

Table 5 Directional total and hemispherical total emissivities of Aeroglaze Z306 in the wavelength range from 5 μm to 16.6 μm at 25 $^{\circ}\text{C}$ and from 4 μm to 20 μm at 150 $^{\circ}\text{C}$ with their corresponding standard uncertainties

Angle	Aeroglaze Z306 ε (25 $^{\circ}\text{C}$)	$u(\varepsilon)$ ($k=1$)	Aeroglaze Z306 ε (150 $^{\circ}\text{C}$)	$u(\varepsilon)$ ($k=1$)
10 $^{\circ}$	0.924	0.012	0.9638	0.0054
20 $^{\circ}$	0.911	0.013	–	–
30 $^{\circ}$	0.919	0.013	0.9615	0.0053
40 $^{\circ}$	0.923	0.012	–	–
50 $^{\circ}$	0.922	0.013	0.9472	0.0052
60 $^{\circ}$	0.888	0.015	–	–
70 $^{\circ}$	0.818	0.013	0.8579	0.0049
ε_{hem}	0.881	0.013	0.9229	0.0052

Table 6 Directional total and hemispherical total emissivities of Aeroglaze Z306 at three different thicknesses. All measurements were taken at a temperature of 150 $^{\circ}\text{C}$ and in the wavelength range from 14.7 μm to 100 μm

Angle	Aeroglaze Z306, 44 μm ε (150 $^{\circ}\text{C}$)	$u(\varepsilon)$ ($k=1$)	Aeroglaze Z306, 99 μm ε (150 $^{\circ}\text{C}$)	$u(\varepsilon)$ ($k=1$)	Aeroglaze Z306, 236 μm ε (150 $^{\circ}\text{C}$)	$u(\varepsilon)$ ($k=1$)
10 $^{\circ}$	0.8793	0.0066	0.9434	0.0102	0.9553	0.0054
30 $^{\circ}$	0.8852	0.0065	0.9422	0.0094	0.9555	0.0054
50 $^{\circ}$	0.8823	0.0066	0.9288	0.0092	0.9402	0.0052
70 $^{\circ}$	0.7966	0.0067	0.8299	0.0082	0.8368	0.0047
ε_{hem}	0.8512	0.0064	0.8971	0.0101	0.9129	0.0052

document ECSS-Q-70-25A [13] with thicknesses of 44 μm , 99 μm and 236 μm . The measurements were taken at a temperature of 150 $^{\circ}\text{C}$ and are shown in Fig. 5 for an angle of observation of 10 $^{\circ}$. A significant decrease in emissivity above 22 μm can be seen for the sample with a coating thickness of 44 μm . The sample with the coating thickness of 236 μm shows a nearly constant (spectrally flat) emissivity. The clearly visible modulation in the emissivity of all three samples for longer wavelengths is explained by an onset of transparency of the coating toward longer wavelengths and multiple beam interference within the coating due to the highly reflective copper substrate. The observed modulation period is inversely proportional to the optical thickness of the coating.

The Aeroglaze Z306 coating of all three thicknesses is fully opaque in the MIR range, but the directional spectral emissivity shows a slight temperature dependence as shown in Fig. 6. The directional spectral emissivity at 25 $^{\circ}\text{C}$ is shown as the brown curve with the corresponding uncertainty range plotted as the shaded area around the curve. The green curve in Fig. 6 illustrates the directional spectral emissivity at 150 $^{\circ}\text{C}$.

Tables 5 and 6 provide the numerical values of the directional total and hemispherical total emissivities of Aeroglaze Z306.

4.4 Acktar Fractal Black

Acktar Fractal Black is a highly emitting coating of the company “Acktar” [14]. Measurements of its reflectivity and other characteristics of this coating can be found in [14, 15], but direct emissivity measurements are missing. Here, the directional spectral emissivity of Acktar Fractal Black was measured under vacuum from 4 μm to 20 μm

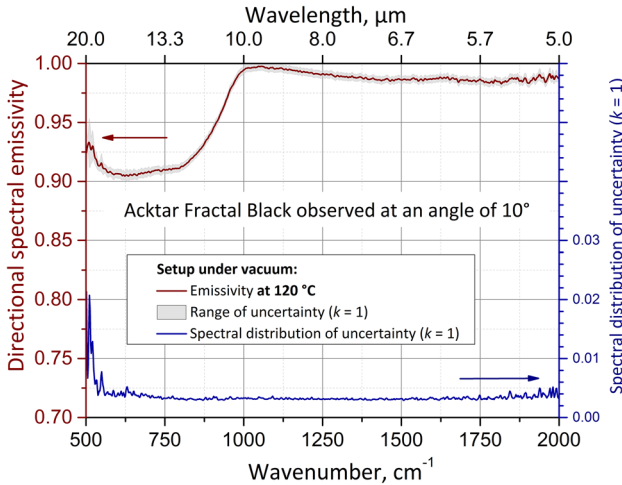


Fig. 7 Directional spectral emissivity of Acktar Fractal Black from 5 μm to 20 μm measured at a temperature of 120 $^{\circ}\text{C}$ and under an angle of observation of 10 $^{\circ}$ with respect to the surface normal. The spectral distribution of the standard uncertainty is shown in the lower half of the plot with the respective scale on the right-hand ordinate axis

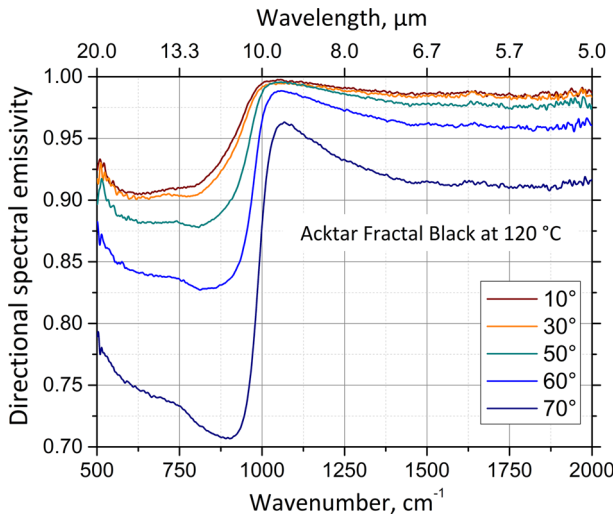


Fig. 8 Directional spectral emissivity of Acktar Fractal Black under different angles of observation with respect to the surface normal

Table 7 Directional total and hemispherical total emissivities of Acktar Fractal Black in the wavelength range from 5.7 μm to 20 μm at 25 $^{\circ}\text{C}$ and from 4 μm to 20 μm at 120 $^{\circ}\text{C}$ with their corresponding standard uncertainties

Angle	Acktar Fractal Black ε (25 $^{\circ}\text{C}$)	$u(\varepsilon)$ ($k=1$)	Acktar Fractal Black ε (120 $^{\circ}\text{C}$)	$u(\varepsilon)$ ($k=1$)
10 $^{\circ}$	0.963	0.017	0.9603	0.0036
20 $^{\circ}$	0.962	0.018	0.9604	0.0037
30 $^{\circ}$	0.962	0.018	0.9565	0.0043
40 $^{\circ}$	0.958	0.018	0.9513	0.0037
50 $^{\circ}$	0.948	0.017	0.9432	0.0038
60 $^{\circ}$	0.919	0.017	0.9134	0.0038
70 $^{\circ}$	0.847	0.017	0.8409	0.0039
ε_{hem}	0.924	0.017	0.9104	0.0038

Table 8 Directional total and hemispherical total emissivities of Acktar Fractal Black with their corresponding standard uncertainties. The measurements were taken at a temperature of 120 $^{\circ}\text{C}$ and in the wavelength range from 20 μm to 100 μm

Angle	Acktar Fractal Black ε (120 $^{\circ}\text{C}$)	$u(\varepsilon)$ ($k=1$)
10 $^{\circ}$	0.928	0.018
30 $^{\circ}$	0.930	0.018
50 $^{\circ}$	0.911	0.018
70 $^{\circ}$	0.780	0.018
ε_{hem}	0.895	0.018

at 120 $^{\circ}\text{C}$. The measurement under an angle of observation of 10 $^{\circ}$ is plotted in Fig. 7. The spectral distribution of the uncertainty is also shown in the lower half of Fig. 7 with the corresponding ordinate axis on the right-hand side. The directional spectral emissivity was also measured under different angles of observation from 10 $^{\circ}$ to 70 $^{\circ}$ and is plotted in Fig. 8. Tables 7 and 8 provide the numerical values of the directional total and hemispherical total emissivities of Acktar Fractal Black.

4.5 Total and Hemispherical Emissivities

The integrated quantities, total and hemispherical emissivity, of the four black coatings are presented here for an overview, depending on temperature and the integrated wavelength range (MIR: 4 μm to 20 μm , FIR: 20 μm to 100 μm). The directional total emissivities with their standard uncertainties are plotted in Figs. 9 and 10 and the hemispherical total emissivities in Fig. 11.

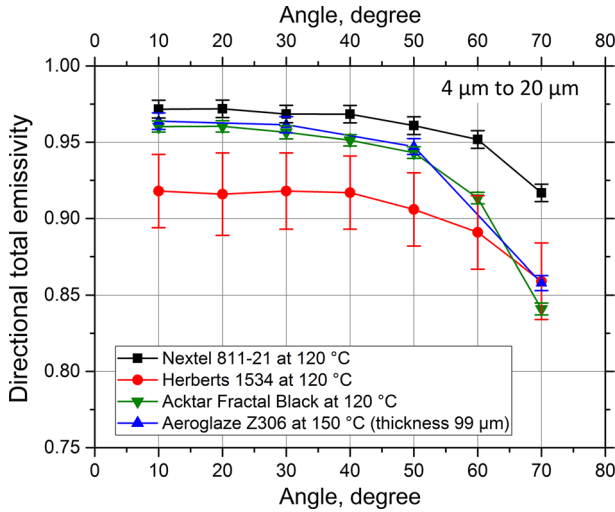


Fig. 9 Directional total emissivities of the investigated coatings in the wavelength range from 4 μm to 20 μm at the temperatures of 120 °C, respectively, 150 °C with their corresponding standard uncertainties

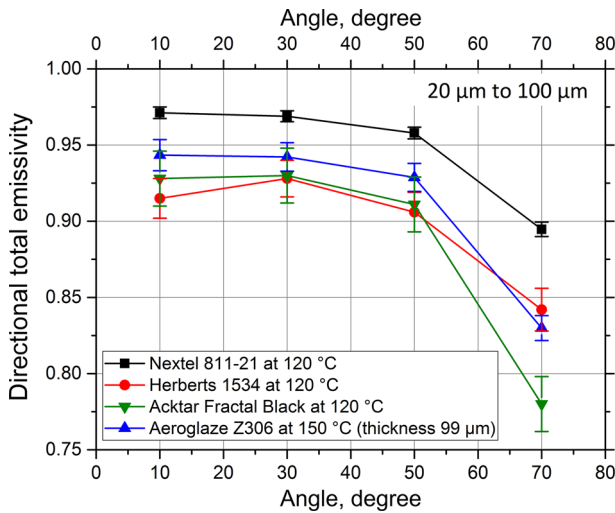


Fig. 10 Directional total emissivities of the investigated coatings in the wavelength range from 20 μm to 100 μm at the temperatures of 120 °C, respectively, 150 °C with their corresponding standard uncertainties

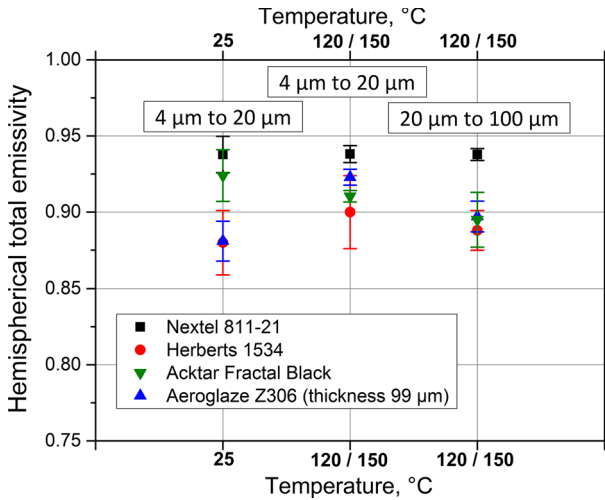


Fig. 11 Hemispherical total emissivities of the investigated coatings with their corresponding standard uncertainties. The results are grouped according to the integrated spectral ranges and measurement temperatures

5 Conclusion

Highly accurate measurements of directional spectral, directional total and hemispherical total emissivities for four widely used black coatings—Nextel 811-21, Herberts 1534, Aeroglaze Z306 and Acktar Fractal Black—were taken by PTB in the wavelengths range from 4 μm to 100 μm at different temperatures in the range from 25 $^{\circ}\text{C}$ to 150 $^{\circ}\text{C}$.

The achieved absolute standard uncertainty ($k = 1$) is calculated according to [5–7]. It is 0.005 or better for measurements at high temperatures ($T = 120$ $^{\circ}\text{C}$ and $T = 150$ $^{\circ}\text{C}$) and it is better than 0.022 (for some measurements better than 0.011) for measurements at 25 $^{\circ}\text{C}$. It should be noted that the achieved uncertainty significantly depends on the experimental conditions and the investigated coating.

The results achieved in this work are traceable to the International Temperature Scale of 1990 (ITS-90) due to the use of two radiance standards in terms of two reference blackbodies which are directly linked to the ITS-90. Furthermore, some of the measurements at the RBCF were validated by comparing them with measurements performed at EMAF. EMAF has successfully participated in CCT-S1, the supplementary comparison of CCT for spectral emissivity [4]. All emissivity results obtained at the RBCF and at the EMAF are consistent within the uncertainties of the measurements.

Note

The spectral emissivity data of the investigated coatings is made available as an electronic supplement to this article on the journals website.

Acknowledgements The authors would like to thank the two anonymous reviewers for their valuable suggestions to the paper.

Open Access This article is distributed under the terms of the Creative Commons Attribution 4.0 International License (<http://creativecommons.org/licenses/by/4.0/>), which permits unrestricted use, distribution, and reproduction in any medium, provided you give appropriate credit to the original author(s) and the source, provide a link to the Creative Commons license, and indicate if changes were made.

References

1. C. Monte, B. Gutschwager, S.P. Morozova, J. Hollandt, *Int. J. Thermophys.* (2009). doi:[10.1007/s10765-008-0442-9](https://doi.org/10.1007/s10765-008-0442-9)
2. A. Adibekyan, C. Monte, M. Kehrt, B. Gutschwager, J. Hollandt, *Int. J. Thermophys.* (2015). doi:[10.1007/s10765-014-1745-7](https://doi.org/10.1007/s10765-014-1745-7)
3. C. Monte, J. Hollandt, *High Temp. High Press.* **39**, 151–164 (2010)
4. Key and supplementary comparisons, CCT-S1, <http://kcdb.bipm.org>
5. Joint Committee for Guides in Metrology (JCGM), Evaluation of measurement data-guide to the expression of uncertainty in measurement, <http://www.bipm.org/en/committees/jc/jcgm/>. Accessed 2008
6. C. Monte, J. Hollandt, *Metrologia* (2010). doi:[10.1088/0026-1394/47/2/s14](https://doi.org/10.1088/0026-1394/47/2/s14)
7. A. Adibekyan, High-accuracy spectral emissivity measurement for industrial and remote sensing applications. (2016), <http://elpub.bib.uni-wuppertal.de/edocs/dokumente/fbc/physik/diss2016/adibekyan>
8. Companies website: <http://www.nextel-coating.com/>
9. J. Lohrengel, R. Todtenhaupt, *PTB-Mitteilungen* **106**, 259–265 (1996)
10. M. Battuello, S. Clausen, J. Hameury, P. Bloembergen, Conference proceedings. TEMPMEKO, 601–606 (1999)
11. M. Persky, *Rev. Sci. Instrum.* (1999). doi:[10.1063/1.1149739](https://doi.org/10.1063/1.1149739)
12. P.G. Maloney, P. Smith, V. King, C. Billman, M. Winkler, E. Mazur, *Appl. Opt.* (2010). doi:[10.1364/AO.49.001065](https://doi.org/10.1364/AO.49.001065)
13. ECSS, European Space Agency, The application of the black coating Aeroglaze Z306, ECSS-Q-70-25A (1999)
14. Technical information on companies website: <http://www.acktar.com/category/BlackOpticalCoating>
15. Y. Salomon, N. Sternberg, I. Gouzman, G. Lempert, E. Grossman, D. Katsir, R. Cotostiano, T. Minton, in *Proceedings of the International Symposium on Materials in a Space Environment*, 2009